Cardiovascular Engineering and Technology, Vol. 5, No. 1, March 2014 *(© 2013)* pp. 82–95
DOI: 10.1007/s13239-013-0169-z

BMES BIOMEDICAL ENGINEERING SOCIETY™ www.bmes.org

Optimization of Oxygen Delivery in Fluid Resuscitation for Hemorrhagic Shock: A Computer Simulation Study

JAMAL SIAM,[1] YOSSI MANDEL,[1,2] and OFER BARNEA[1]

[1]Department of Biomedical Engineering, Tel Aviv University, 69978 Ramat Aviv, Israel; and [2]The Mina & Everard Goodman Faculty of Life Sciences, Bar Ilan University, Ramat Gan, Israel

(Received 18 November 2012; accepted 26 October 2013; published online 8 November 2013)

Associate Editor Ajit P. Yoganathan oversaw the review of this article.

Abstract—The main objective of fluid resuscitation in hemorrhage induced hypovolemia is to increase oxygen delivery to vital organs and to restore other hemodynamic variables to acceptable physiological range. Since replacement of blood with fluid causes both increase in cardiac output and decrease in the plasma oxygen carrying unit concentration, there is an overall opposing effect on total oxygen delivery rate to tissue. Thus, optimal fluid infusion rate and volume may be expected. The purpose of this study was to study the temporal dynamics of oxygen delivery rate during fluid replacement in a controlled hemorrhage scenario and seek these optimal values. A hemodynamic model of the human adult cardiovascular system was developed to simulate and evaluate arterial oxygen delivery at normal and at hemorrhagic conditions in different fluid resuscitation regimes. The results demonstrated the existence of a unique optimal fluid replacement regimen for maximal oxygen delivery rate at different controlled bleeding scenarios. The maintenance of high oxygen delivery rate was better with lower fluid infusion rates. The model results indicate that hematocrit and mean arterial pressure can be used to determine the optimal infusion rate and fluid infusion endpoint in fluid resuscitation.

Keywords—Hemorrhage, Trauma, Fluid replacement, Computer simulation, Oxygen delivery.

INTRODUCTION

According to the World Health Organization (WHO) report, more than 10% of the world's deaths in 2010 were caused by injuries from car accidents, military combat and other types of violence.[35] Bleeding and hemorrhagic shock are the major triggers of death or permanent organ dysfunction in most injured patients. Early and advanced treatment has been shown to increase survival in trauma patients.[1] Hemorrhage induced hypovolemia goes through a cascade of events that involves changes in hemodynamic parameters and blood composition eventually leading to decrease in oxygen delivery to cells, causing cell necrosis and organ malfunction.[8] Hemorrhagic shock has been classified into four classes according to the volume of blood loss and patient physiological symptoms.[1] Hemorrhagic shock was further classified into controlled and uncontrolled hemorrhagic shock (CHS and UCHS). In CHS, the cause of bleeding can be identified and controlled immediately and treatment can be provided immediately after the termination of the bleeding. In UCHS, bleeding cannot be terminated and treatment is given in parallel with continuous blood loss, until patient is being transferred to higher level care where definite treatment is given. Several trauma care expert teams, such as the American Advanced Trauma Life Support (ATLS) team,[1] the British National Institute for Clinical Excellence (NHS)[21] and others have developed guidelines for pre-hospital injury management; fluid resuscitation guidelines being one of the most important components of treatment. The infusion of resuscitation fluid aims at restoring tissue perfusion and oxygen delivery to cells by replacing blood volume loss with fluid.

However, this treatment is far from being optimal, as loss of oxygen carrying units (red blood cells) are replaced with fluids with no oxygen carrying capacity. Since the establishment of fluid treatment as a resuscitation procedure during the World War II many controversies have risen. This has stimulated researchers from the animal, clinical and engineering fields to search for an optimal fluid resuscitation protocol. One of the main points of controversies is the type of replacement fluid (colloids vs. crystalloids).[6,9,25] Other open issues are optimal volume and rate of fluid

Address correspondence to Ofer Barnea, Department of Biomedical Engineering, Tel Aviv University, 69978 Ramat Aviv, Israel. Electronic mail: barneao@eng.tau.ac.il

Jamal Siam and Yossi Mandel share equal contribution to the paper.

replacement. ATLS guidelines recommend an initial rapid infusion of 1–2 L of warmed isotonic electrolyte solutions such as normal saline (NS) or lactated Ringer's solution using boluses of 250 mL.[1] The NHS recommends the use of crystalloid fluid resuscitation in absence of radial pulse in boluses of no more than 250 mL. The patient should then be reassessed and the process repeated until a radial pulse is palpable. Both guidelines do not clearly define the appropriate rate and amount of fluid infusion. A clinical meta-analysis found that there was no evidence against the use of early or larger volume of fluid administration.[15] Various animal models were developed to assess the effect of fluid volume and rate on mortality and re-bleeding,[5,14,24,30] but the optimal fluid resuscitation protocol is still under debate.

Mathematical modeling has also been used to better understand and estimate physiological parameters in various hemorrhage and fluid resuscitation scenarios. Guyton and Coleman[10] used computer simulation to study the long-term regulation of the circulation. Boyer *et al.*[4] developed a model to simulate the human cardiovascular system response to changes in posture, blood loss, transfusion and automatic blockade. Mardel *et al.* simulated the events occurring during first 2 h of hemorrhage and compared their results to available data in the literature. They found that transcapillary refill and hemodilution were in good correlation with experimental data.[18] The model was then extended to study hemodilution and blood pressure responses to fluid infusion, and it allowed multiple infusions of various fluids to be specified while estimating the volumes added by transcapillary refill. The model was useful for assessing the effects of various treatment scenarios on a range of physiological parameters in hypovolemic shock.[29] Gyenge *et al.*[11] developed a compartmental model that formulated short term whole body fluid, protein, and ion distribution and transport. The model was tested against data available in the literature for three different saline solutions. Model predictions were in good agreement with the experimental data.[12] Hedlund *et al.*[13] developed a model for the prediction of important clinical variables, in pathological conditions, based on variable settings of fluid and losses inputs. Barnea and Sheffer[2] used computer simulation to study the effect of fluid infusion on myocardial oxygen balance, and found that hemodilution contributes to myocardial oxygen deficit. Mazzoni *et al.*[19] developed a model to study the effects of various resuscitation fluids and found that hyperosmotic solution restored blood volume most efficiently, but it had the adverse effect of increasing the bleeding rate in uncontrolled hemorrhage. Secomb *et al.*[27,28] studied and modeled the microcirculation system, while exploring the various humoral, neural and metabolic effects on the microcirculatory perfusion. Lodi and Ursino[17] modeled the hemodynamic effect of cerebral vasospasm. The model simulated some clinical results, reported in literature, concerning the patterns of middle cerebral artery velocities. Model predictions were in fair agreement with the clinical data. Simulation results showed that false negative results might be induced if vasospasm is assessed merely through velocity measurements performed by the transcranial Doppler technique. Ursino and Magosso studied the effect of tissue hypoxia on cerebrovascular regulation and showed that their model was able to predict and reproduce the patterns of pial artery caliber and cerebral blood fluid under a large variety of physiological stimuli. It could also explain the experimental results of hemodilution on cerebral blood flow.[33] Stevens and Lakin[31] developed a mathematical model with logistically defined nervous system regulatory mechanisms. The model was capable of accurately describing the pressure, volume, and flow dynamics of the systemic circulatory system over the full physiological range of human pressures and volumes. Model predictions were in near-perfect agreement with the experimental observations of hemodynamic parameters in the case of significant hemorrhage.

The present mathematical-model study was planned to explore optimization of fluid volume and infusion rate according to maximum tissue oxygen delivery rate D_{O_2}. The second goal was to define an end point of fluid administration using available clinical markers that can be monitored during fluid resuscitation and help to predict the maximum value of D_{O_2}. The physiological basis for the existence of such an optimal point is the opposing effects of fluid administration on the two major parameters determining oxygen delivery, i.e., cardiac output (CO) and hematocrit (HCT). While on one hand volume replacement increases CO, and thus increases oxygen delivery rate, it also decrease HCT level, which results in decreased oxygen delivery rate. In a previous mathematical model we demonstrated a similar effect on cardiac oxygen balance where oxygen deficit occurred following fluid infusion that had increased the workload of the heart without adequate increase in oxygen supply.[2]

The present study analyzed the temporal dynamics of tissue oxygen delivery rate during fluid replacement therapy in order to find a fluid replacement protocol (infusion rate and volume) where maximal oxygen is delivered continuously. The model also studied the effect of fluid type (crystalloids or colloids) on the hemodynamic response and oxygen delivery. We hypothesized that there is an optimal value oxygen delivery where fluid administration should be interrupted. This point can be established in the field using

the two main determinant of oxygen delivery, namely HCT and mean arterial pressure (MAP).

MATERIALS AND METHODS

The cardiovascular model is presented in Fig. 1. The methodology of the model design was based on previously published models.[2] The new model is briefly described while all details are given in the Appendix. The model was developed to represent major relevant hemodynamic phenomena. It takes into a count the distribution of blood to different vital and non-vital organs, the interaction among the various parts of the vascular tree, the distribution of blood pressure, flow and oxygen flow in the various parts of the cardiovascular system. The mathematical model of the human cardiovascular system and simulation programs were developed in MATLAB (Mathwork Company, version 10) environment and included a cardiovascular compartment, an interstitial compartment, and fluid exchange between these two compartments.

The model of fluid exchange between the cardiovascular and the interstitial compartments followed the Starling equation.[7] Bleeding and fluid resuscitation models were then added to simulate the effect of fluid treatment on tissue oxygen delivery.

The cardiovascular model was designed to generate the hemodynamic response for the different blood loss and fluid resuscitation conditions. The hemodynamic equations are presented in the Appendix and are briefly described here. The model is composed of the heart, a sub tree of the systemic circulation, a sub tree of the pulmonary circulation and an interstitial compartment. This level of detail can adequately simulate the load, flow, and CO as well as pressure levels at the capillary beds which are required to obtain realistic fluid transfer rate between the intravascular and interstitial compartments. In addition, the model can predict flow distribution to vital and non-vital organs.

Mathematical and structural aspects of the model are presented in the Appendix in two tables. The heart was constructed of four compliant chambers and four resistive unidirectional valves (Tables A1 and A2). The equations in Table A1 were used to determine pressure, flow, and volume relations of each chamber during the different phases of the cardiac cycle.

The model of the vascular system was a multi-element model (Fig. 1). It was aimed at predicting the distribution of blood, fluids and oxygen delivery rate to the various vital and non-vital. The aorta was divided into nine segments; the first two segments represent the aortic root and the arch of the aorta respectively. The thoracic aorta was modeled by the following four segments and the abdominal aorta by the last three segments. Each aortic segment was modeled by a three elements circuit representing viscous forces, fluid inertia and vessel compliance. Seven branches were derived from the aorta. The coronary

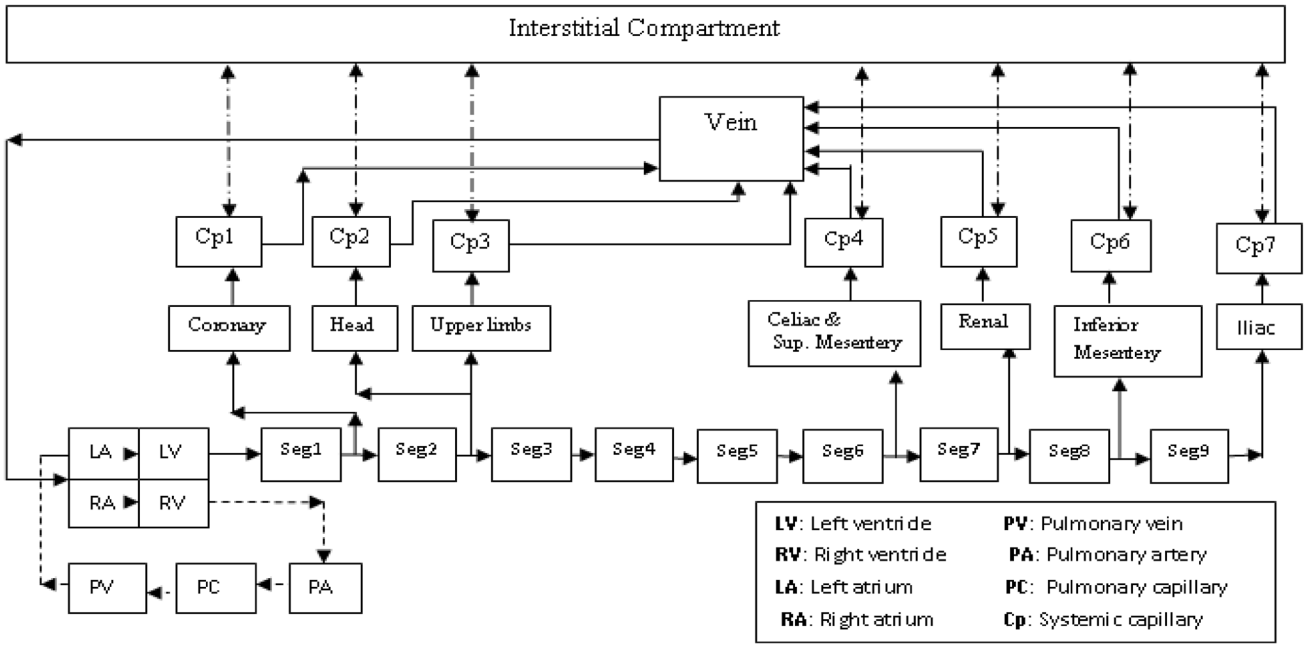

FIGURE 1. Model structure: intravascular and interstitial compartments.

artery branched from the aortic root. The head and upper limbs equivalent arteries branched from the arch of the aorta. The celiac and upper mesenteric equivalent artery branched from the end of the thoracic artery. The renal, inferior mesenteric and iliac arteries were derived from the end of the first, second, and third abdominal segments respectively. Each arterial segment was terminated with a capillary equivalent resistor that connected the artery to the systemic vein. The systemic arteries and the systemic vein were represented by two-element models where fluid mass and acceleration forces were neglected.[34] Elements representing viscous forces were calculated as functions of HCT, thereby reducing resistance to flow for diluted blood.[20]

The pulmonary sub-tree was modeled with three segments that represented the pulmonary artery, capillary bed, and vein. Two-element models were used (inertia neglected) in each of the pulmonary segments.

To determine the fluid shifts between the different fluid compartments, it was necessary to add a model of the interstitial space. The model took into account the relations between the interstitial fluid (ISF) volume, the hydrostatic pressure developed by this volume, and the oncotic pressure exerted by its colloids concentration. These relations are similar to those previously used in Barnea and Sheffer.[2] The fluid exchange process considered only the balance of forces at the capillary arterial-end and venous-end. The lymphatic system and the lymph return were not included in this model.

The initial total blood volume considered in the model was 5.6 L.[16] The initial total ISF volume at the normal operating conditions was assumed to be 12 L. We assumed that changes in the ISF volume can occur only by the shift of fluid between the intravascular space and the interstitium. Permeability to fluid of the capillary–interstitium barrier was assumed to be constant and independent of the state of shock. The barrier was also assumed to be completely impermeable to colloids.

The bleeding included loss of fluid, red blood cells, and colloids. Level of hemorrhage was a function of the hydrostatic blood pressure at the arterial end of the capillary and the resistance to flow that was altered to control the class of hemorrhage (Appendix Table A2). The resuscitation fluid was injected into the systemic vein. Two different fluids, NS and dextran-70 6%, were used as pilot solutions to study the effect of crystalloids and colloids fluid on the dynamics of oxygen delivery.

In the oxygen delivery process, no distinctions were made between the mechanisms of oxygen transport. The computation of the oxygen concentration in a deciliter of blood was based on the set of equations (Eq. (1)).

$$\begin{aligned} [O_2] &= \alpha \times P_{O_2} + [HbO_2] \\ [Hb] &= HCT \times [Hb_{RBC}] \\ [HbO_2] &= SaO_2 \times HbO_{2\_max} \times [Hb], \end{aligned} \tag{1}$$

where α is the oxygen solubility coefficient in blood, $[O_2]$ is the total oxygen concentration, $[HbO_2]$ is the concentration of oxygen bounded to hemoglobin, P_{O_2} is the oxygen partial pressure, SaO_2 is the saturation of hemoglobin, [Hb] is the hemoglobin mass density in deciliter of blood, $[Hb_{RBC}]$ is the hemoglobin mass density in deciliter of red blood cells, and HbO_{2_max} is the maximum oxygen carrying capacity. The oxygen concentration is $[O_2] = 20.3\ mLO_2/dL$ for typical values: $\alpha = 0.0024\ mLO_2/dL\ mmHg$, $HCT = 0.44$, $[Hb_{RBC}] = 34\ g/dL$, $HbO_{2\_max} = 1.34\ [mLO_2/gr\_Hb]$, $P_{O_2} = 100$ mmHg, and 100% saturation.

In the model, total oxygen content was calculated as the sum of oxygen dissolved in blood and oxygen carried by RBCs. The hemoglobin molecules in the systemic arteries were assumed to be fully saturated with oxygen, and so the concentration of oxygen in the unit volume of RBCs was considered constant during all the simulation tasks.

Oxygen delivery rate (D_{O_2}) as a function of CO at any time t is computed by:

$$D_{O_2}(t) = [O_2(t)] \times CO(t). \tag{2}$$

Model and simulation were used to study the normal hemodynamic response, bleeding phase, bleeding control and monitoring phase without treatment, fluid resuscitation phase, and follow up phase.

Classes II, III, and IV hemorrhage were modeled to study their effect on the hemodynamic variables. In all the cases the rate of bleeding was a function of the average pressure at the capillary arterial-end and a controlled bleeding resistance (Appendix Eq. (9)).

The simulation sequence was repeated for the different classes of hemorrhage with a wide range of infusion rates (40, 60, and 80 mL/min) for NS and dextran-70 6%.

RESULTS

Validation of Initial Conditions

Validation of the model initial conditions was done by comparing the simulation steady state pressures (Fig. 2), flow, HCT, net filtration, and oxygen delivery rate to normal physiological data, as shown in Table A3. The simulation results of the left ventricle and aortic pressures (Fig. 2a) and left ventricle flow

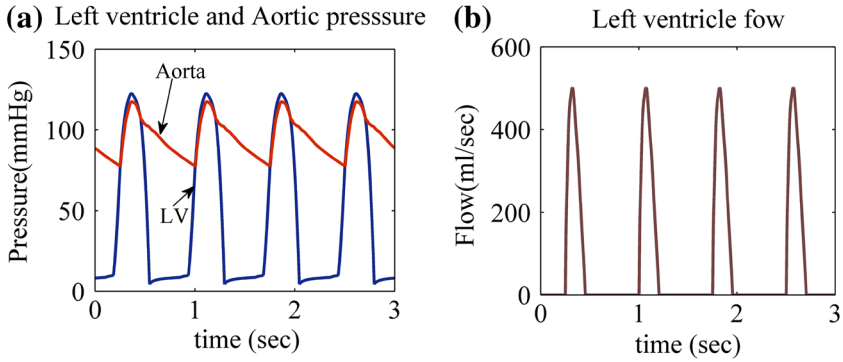

FIGURE 2. Hemodynamics in the left ventricle and the aorta. (a) The pressure curves in LV and aorta. (b) LV flow.

(Fig. 2b) were in the range of normal physiological values. Steady state MAP was 91.6 mmHg, and the oxygen delivery rate was 1116 mL/min. The steady state net fluid filtration was approximately balanced, as expected.

Hemodynamic Effects of Various Bleeding Rates with No Fluid Infusion

The initial bleeding rates (BLDR) were 52.7, 81, and 161.6 mL/min for classes II, III, and IV, respectively, and it decreased gradually as blood pressure dropped during the bleeding period to rates of 70, 58, and 37% of the initial rates (Fig. 3a). The total blood losses for the selected bleeding resistances in the three classes of hemorrhage (class II, III, and IV) were 1100, 1540, and 2420 mL, respectively. Arterial blood pressure decreased to 72, 61, and 40% of normal values following hemorrhage classes II, III, and VI, respectively (Fig. 3b). Following the control of hemorrhage, MAP increased asymptotically to values of 79, 64, and 48% of the normal value due to fluid reabsorption.

At the time of hemorrhage control, HCT reached levels of 42.6, 41.8, and 40% for the classes II, III, and IV, respectively (Fig. 3c), and continued to decrease due to net influx of fluid. At steady state, HCT levels reached minimum values of 40.6, 39.1, and 35.7%, respectively. The resulting hypovolemia caused a reduction in the preload and stroke volume of the heart compromising its function. The left ventricle PV-loops were shifted to left and by the time of hemorrhage control (Fig. A1) ejection fractions were reduced to 81, 77.8, and 66.7% from the pre bleeding value for the classes II, III, and IV, respectively. The reduction of ejection fraction and consequent heart work became more evident for higher hemorrhage levels.

Bleeding also caused a marked decrease in oxygen delivery rate down to 67, 54, and 33% of the normal steady state value for hemorrhage classes II, III, and IV, respectively. Oxygen delivery rates were slightly increased following the control of hemorrhage and reached asymptotic values of 70, 60, and 39% of the normal steady state value for the classes II, III, and IV, respectively. The increase in oxygen delivery rates were caused by fluid reabsorption from the interstitial compartment and the following increase in intravascular volume, pressure and CO (data not shown).

Hemodynamic Effects of Fluid Infusion

Infusion of both NS (Fig. 4) and dextran (Fig. 5) caused a significant increase in blood pressure in parallel with marked reduction in HCT. In NS, approximately 72% of infused volume escaped out of the intravascular space into the interstitium as compared to only 7.5% in the case of dextran. Accordingly, the decrease in HCT and the increase in MAP were faster in dextran than those obtained for the NS (Figs. 4b, 4c, 5b, and 5c). Higher infusion rates induced a more substantial increase in blood volume and arterial pressures, while HCT decreased faster. After the termination of fluid infusion, intravascular fluid volume continued to filtrate into the ISF compartment resulting in decrease of blood volume and MAP while the HCT increased, the effect was significantly larger for saline (Figs. 4a–4c) as compared to dextran (Figs. 5a–5c).

Effects of Infusion Rate and Fluid Type on Oxygen Delivery Rate

The time-dependent pattern of the oxygen delivery rate was similar between all classes of hemorrhage and fluid infusion rates for both NS (Fig. 6) and dextran solutions (Fig. 7). Fluid treatment caused a significant increase in oxygen delivery rates up to a maximum that was lower for higher bleeding volume (905, 821, and 650 mLO_2/min for the classes II, III, and IV, respectively). Interestingly, similar values of maximum delivery rates were obtained for all three infusion rates,

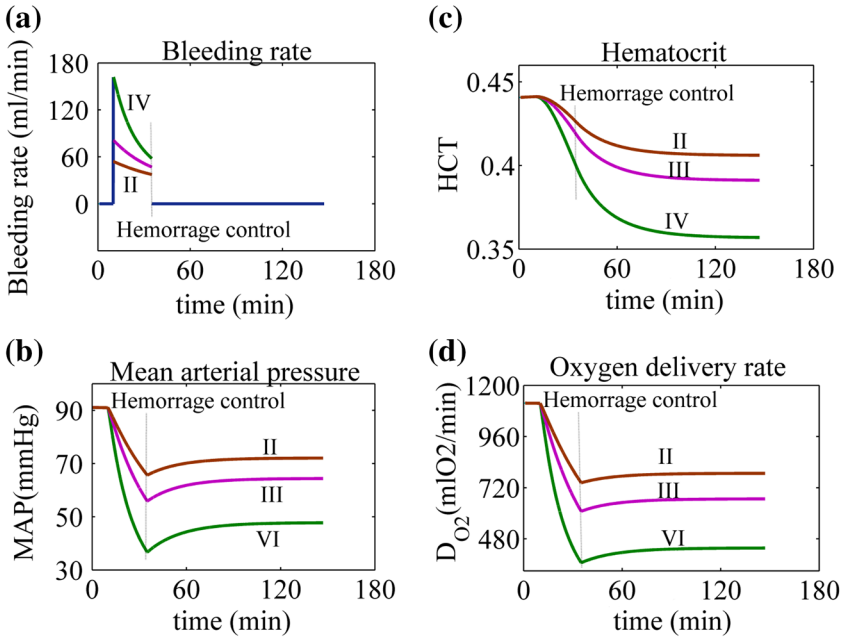

FIGURE 3. Bleeding rate: (a) mean arterial pressure, (b) hematocrit (c), and oxygen delivery rate (d) for three hemorrhage classes (II, III, IV) in a controlled hemorrhage scenario with no fluid treatment.

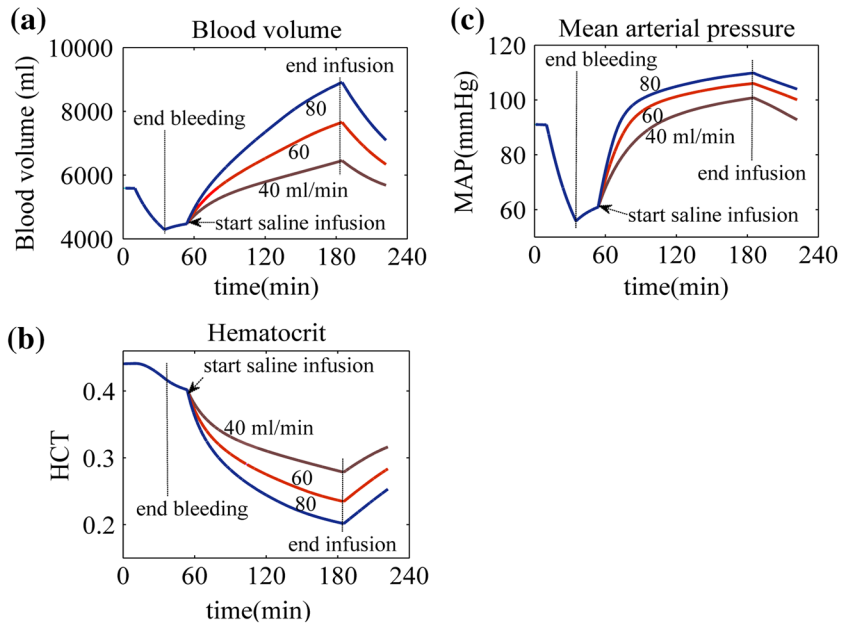

FIGURE 4. Intravascular volume (a), mean arterial pressure (b), and hematocrit (c) during saline infusion in class III controlled hemorrhage.

however, higher infusion rates were associated with earlier appearance of that maximum, and the difference in time was larger for higher bleeding classes with NS (Fig. 6). The maximal oxygen delivery rate point was followed by a continuous decrease which was faster for higher infusion rates and continued to decrease as long as fluid was administrated. Following discontinuation of fluid infusion, there was a second increase in oxygen delivery rate, which was caused by fluid shifts from the intravascular into the interstitial compartment and the resulting HCT increase that caused an increase in oxygen delivery.

The fluid volumes needed to achieve maximal oxygen delivery rate with NS were 1410, 1700, and 2681 mL) for bleeding classes II, III, and IV, respectively, and were significantly smaller (575, 750, and

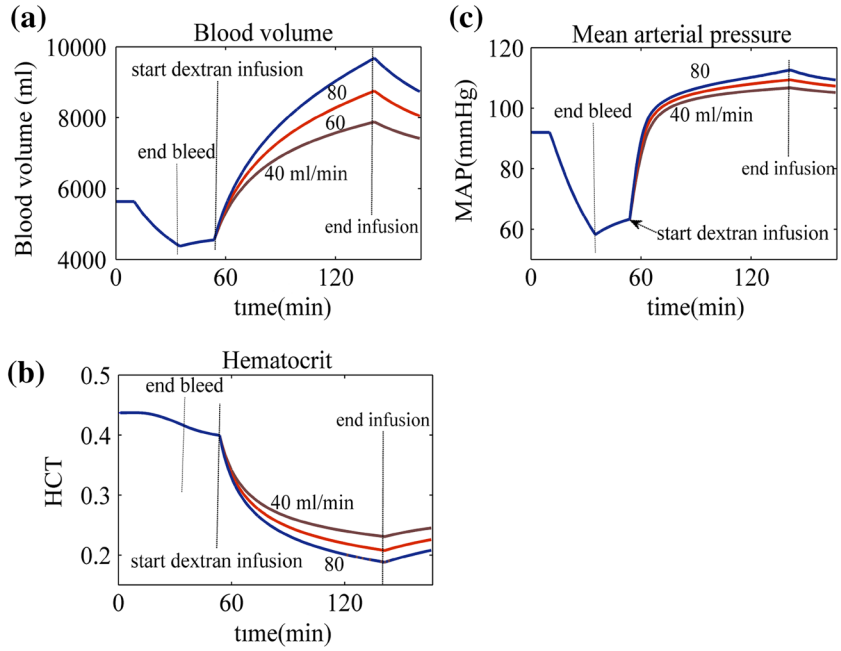

FIGURE 5. Intravascular volume (a), mean arterial pressure (b), and hematocrit (c) during dextran infusion in class III controlled hemorrhage.

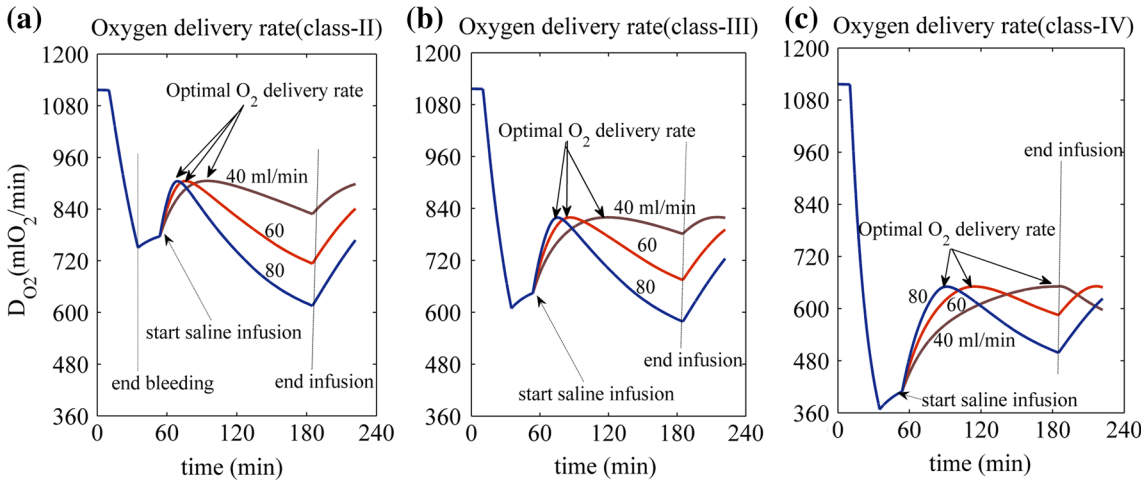

FIGURE 6. Oxygen delivery rate during saline infusion for three classes of hemorrhage.

1311 mL) for dextran infusion. The improvement in oxygen delivery rate, for both NS and dextran, was higher in the case of severe class IV hemorrhage (339 mLO_2/min) as compared to class II hemorrhage (201 mLO_2/min).

Interestingly, for the same bleeding volume (class III), maximum oxygen delivery rates were identical between the two fluid types (821 mLO_2/min). However, since lower dextran volume were required in order to achieve maximal oxygen delivery rate, the optimal point was achieved significantly earlier with dextran treatment (8.2, 9.7, and 11.7 min) as compared to saline (21, 31, and 64 min, Fig. 6), for infusion rates 80, 60, and 40 mL/min, respectively (Fig. 7). When infusion of saline was terminated at the point of maximum D_{O_2}, for the class III hemorrhage (Fig. 8a), oxygen delivery rate decreased and reached a plateau at 87% of the maximum for all the infusion rates. During the transition to steady state, D_{O_2} maintained higher values for slower infusion rates. CO, during a class III hemorrhage and subsequent saline infusion, is shown in Fig. 8b. Infusion was terminated at the maximal D_{O_2} point. CO decreased during hemorrhage and increased during fluid infusion in a non-linear

manner. After the cessation of fluid infusion, CO decreased and reached a plateau at 76% of the maximum for all infusion rates.

Clinical Indicators for Oxygen Delivery Rate Estimation

We found that the oxygen delivery rate has similar time pattern to the HCT × MAP product (HCMP), as shown in Fig. 9a. D_{O_2} was highly correlated with HCMP with goodness of linear fitting >0.98 (D_{O_2} = 2.003 × HCMP-36.72, D_{O_2} = 2.016 × HCMP-37.08, and D_{O_2} = 2.039 × HCMP-37.66 for the infusion rates of 80, 60, and 40 mL/min, respectively). The relation between D_{O_2} and HCMP, during NS infusion up to the maximum HCMP value, is shown in Fig. 9b. The plots of D_{O_2} vs. HCMP almost overlapped during all the course of the infusion process for all infusion rates, small differences between the plots were observed in the vicinity of the maximum HCMP value. The error in oxygen delivery rate when infusion was terminated at the maximum of HCMP instead of maximum D_{O_2} was less than 4% of maximum D_{O_2} value for all the three infusion rates.

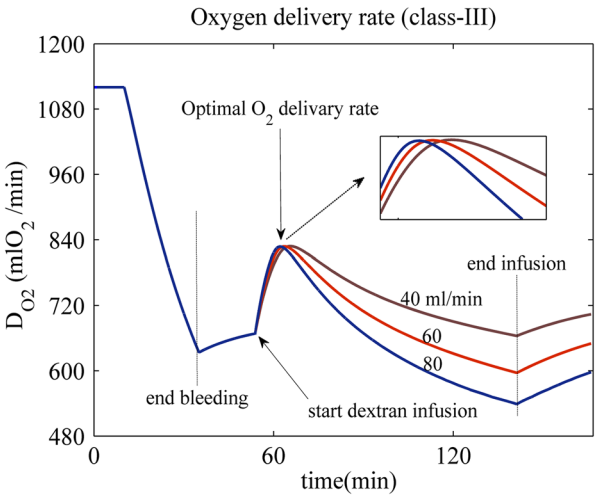

FIGURE 7. Oxygen delivery rate during dextran infusion for class III hemorrhage.

DISCUSSION

Optimization of Infusion Treatment in Controlled Hemorrhage Shock

The goal of fluid resuscitation is to improve oxygen delivery to the various body organs by increasing oxygen delivery capacity and tissue perfusion. Simulation results showed that this goal can be achieved with fluid infusion. However, the increase in oxygen delivery is strictly dependent on the fluid infusion protocol and end point. The simulation results showed the existence of an optimal infusion volume in which a maximal oxygen delivery rate is achieved. Continuing infusion beyond that optimal volume will result in a continuous reduction in oxygen delivery rate to levels that are even lower than pretreatment values (Figs. 6 and 7). Interestingly, cessation of fluid infusion at the maximum oxygen delivery rate point was followed by a transient reduction of the oxygen delivery rate caused by fluid filtration decreasing the intravascular fluid volume (Fig. 8). The slower fluid infusion rates showed a delayed and slower decreasing behavior than that of higher infusion rates, but all the transients finally settled at the same final D_{O_2} value of about 720 mLO_2/min, significantly higher than the values obtained when infusion was continued beyond the optimal point

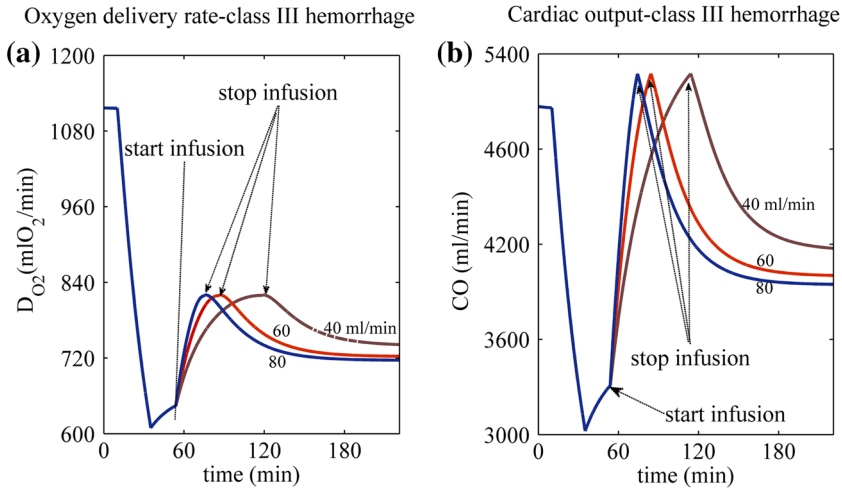

FIGURE 8. Oxygen delivery rate and cardiac output during saline infusion in class III hemorrhage with fluid infusion terminated at the point of maximum D_{O_2}.

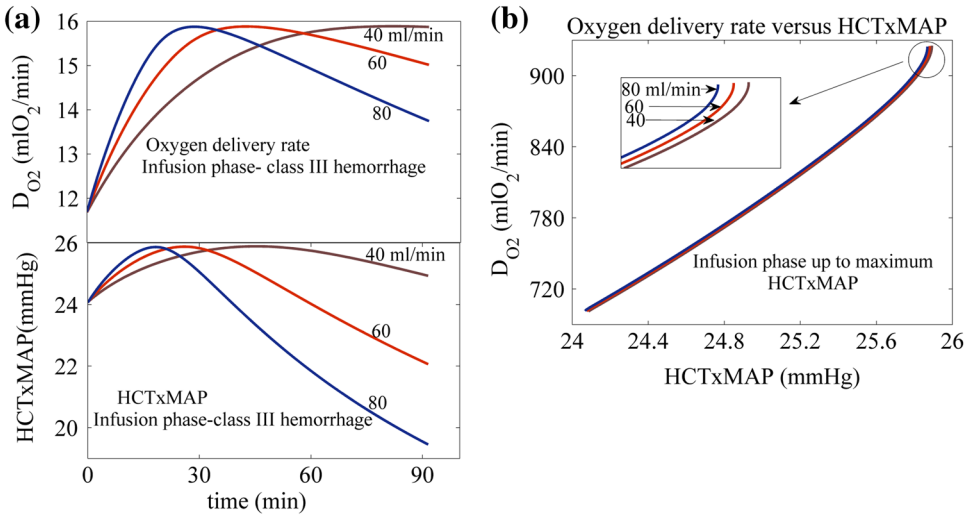

FIGURE 9. (a) HCT × MAP (upper trace) and D_{O_2} (lower trace) are depicted against time during various rates of infusion of normal saline. (b) D_{O_2} against HCT × MAP is shown during saline infusion up to the point of maximum HCT × MAP for various infusion rates.

(down to about 500 mLO_2/min in high fluid infusion rate, Fig. 6c).

The physiological basis for the existence of a maximum for tissue oxygen delivery is the opposite effects of volume replacement on CO and HCT. During first phase of fluid replacement, CO increases rapidly due to increase in preload pressure while HCT decreased linearly, thus the net effect of these two opposing processes is an increase in oxygen delivery rates. However beyond a certain intravascular volume and left ventricle filling volume, CO reaches a plateau, while the continuing blood dilution and resulting decrease in HCT concentration cause a net effect of decrease in D_{O_2}. Interestingly, the simulation results showed that the oxygen delivery rate curve reached a maximal value that was equal for all fluid delivery rates, although this maximum occurred earlier for higher infusion rates. Of importance, the simulation results also demonstrated that with lower infusion rate there is higher tolerance to continuation of infusion beyond the optimal point as compared to higher infusion rate.

The existence of an optimum volume for fluid replacement in a case of CHS calls for the following question: when should the fluid infusion be terminated? The data above shows that fluid replacement caused a marked increase in D_{O_2} up to an optimal point, which was followed by a gradual decrease in D_{O_2} (Figs. 6 and 7). It is thus of great importance to find clinical parameters which will enable the clinician to optimize fluid treatment and stop or change infusion rate when maximal D_{O_2} is achieved.

The simulation showed that the product of two clinically available measurements, namely, HCT and MAP can be used as a reliable index for D_{O_2} estimation. We also found that in cases where continuous monitoring of HCT is not possible, a single measurement of HCT before treatment can give a rough estimate of the optimal fluid for a given fluid rate or type (colloid or crystalloid). In both cases, our results stress the importance of developing a mobile device for field measurements of HCT, such as was recently reported.[32]

Our results suggest that fluid treatment for CHS can be optimize by continuous monitoring of HCT and MAP. Fluid treatment should be given continuously as long as the product MAP × HCT keeps rising and should be stopped when it start to decrease. Following cessation of infusion, HCT × MAP should continue to be monitored and further infusion volume and rates should be adjusted accordingly. The results of Figs. 6, 8a, 9a, and 9b suggest that a plausible resuscitation protocol may use the maximum HCT × MAP point as the point at which fluid resuscitation should switch from high infusion rates to very small rates that aim at maintaining the maximum value of D_{O_2}.

As an alternative method we wanted to estimate if a single HCT measurement at the time of hemorrhage control could give an estimate of the fluid volume needed to achieve maximal D_{O_2}. The optimal rate of fluid infusion could also affect the overall outcome of the treatment. Despite the finding that higher infusion rates achieved the maximal D_{O_2} significantly earlier than lower rates, higher infusion rates also carries larger risk for over treatment and reduced D_{O_2} (Fig. 6) and thus stress the importance of continuous monitoring of HCT–MAP product.

Of interest is the fact that both NS and dextran-70 showed the same maximum oxygen delivery rate.

However, with dextran treatment, maximum D_{O_2} was obtained significantly more rapidly than with NS and with smaller infusion volume (750 vs. 1700 mL) since there is a smaller extravasation volume of dextran out of blood vessels.[23] Nevertheless, similarly to high rates of NS, dextran treatment carries the risk of over treatment leading to a severe reduction in D_{O_2} to levels lower than pre treatment. In fact, 10 min of continuous dextran infusion at a rate of 80 mL/min beyond the maximum point can reduce D_{O_2} by 5.55%, while this value is about 1.7% for NS.

Thus, when administering high infusion rates or giving dextran treatment, it seems that strict monitoring of HCT and MAP are important for optimizing fluid treatment and avoiding over treatment which can lead to deterioration. NS treatment at lower infusion rate is recommended when slower response to treatment can be tolerated or when strict continuous monitoring is not possible. Nevertheless, the present study was not designed to answer the question whether it is clinically better to achieve earlier maximal oxygen delivery rate or to maintain a slower and continuously increasing rate toward a delayed maximum. Thought this question should be answered by clinical or animal research, our study suggests monitoring fluid replacement by simple and available physiological and laboratory parameters.

The dynamic of HCT levels predicted by our model (Fig. 4b) are in agreement with Baue *et al.*[3] who measured HCT and oxygen consumption in dogs following blood volume depletion. They found that volume replacement with Ringer solution was associated with a sharp reduction in HCT, which was followed by a gradual increase up to about 60% of initial values. The larger decrease in HCT levels reported in response to colloids as compared to crystalloids, was also reported by Simpson *et al.*[29]

Natural Compensatory Mechanisms in Hypovolemia

The response to the various levels of hemorrhage without treatment showed a significant decrease in the MAP, CO, and HCT during the bleeding phase which were followed by an increase in MAP and D_{O_2} in parallel to a sharp decrease in HCT (Fig. 3). The simulation result of the MAP and HCT for class III was similar to the simulation result reported in Barnea and Sheffer,[2] and it was in agreement with the experimental results in Yitzchak *et al.*[36] The steady state HCT levels are also in good agreement with clinical data reported by Ryan *et al.*,[26] which showed that HCT levels on admission can predict patients' survival. These phenomena can be explained by a net fluid shifts from the ISF compartment into the cardiovascular compartment leading to increase in CO and MAP in parallel to a diluting HCT. This reabsorption phenomenon was more intense in higher bleeding volume because of larger decrease in MAP and hydrostatic pressure, and partially compensated for the hypovolemia and the decrease of the MAP and CO. However, the effect of this natural compensation mechanism on D_{O_2} was only 3.9, 5.2, and 6.1% for bleeding class II, III, and IV, respectively, and was not significant with respect to the total D_{O_2} reduction caused by hemorrhage or to the improvement of D_{O_2} provided by fluid treatment.

There are several limitations to our study. First, the model does not include various pathophysiological processes occurring during hemorrhagic shock, such as increase in blood vessels permeability[22] or peripheral vasoconstriction, which leads to increased blood pressure and reduces perfusion in peripheral organs. We also didn't include the effect of acidosis, occurring during shock and affecting the Hb dissociation curve and thus affecting the tissue oxygen delivery. Second, our model did not include the effect of various neural and humoral signals affecting the microcirculation perfusion nor it included various effect of the red blood cell membrane on circulation. These effects were extensively studied and reviewed by Secomb *et al.*[27,28] Third, our model deals with controlled hemorrhage, and is thus not applicable for many trauma cases where bleeding is still occurring during fluid treatment. The model also did not included infusion of blood, and is thus more appropriate for cases treated in field before arriving to centers where blood is available. These study limitations call for further analytical and experimental studies.

CONCLUSIONS

The study demonstrated that fluid replacement volume can be optimized in order to achieve maximal oxygen delivery rate in a controlled hemorrhage scenario. The study suggests that continuous monitoring of HCT × MAP product can assist in determining the point where fluid administration should be stopped, or otherwise they will have a detrimental effect on oxygen delivery by blood. Monitoring these parameters could be of even greater importance when high fluid rates or colloid treatment are considered. Our results call for developing field mobile devices for monitoring of HCT levels. Further animal and clinical studies should be conducted to validate our simulation study.

APPENDIX

Fluid Exchange

The fluid exchange model assumes that the concentration of colloids in the interstitial space is constant (2%,[2]) and there is no escape of colloids from the intravascular compartment to the interstitial space; the model also ignores the lymph return. The plasma and RBCs volumes are computed separately. The plasma volume during hemorrhage is computed using Eq. (10) which takes into account the combined effect of the fluid loss through bleeding and the fluid exchange with interstitial space. In this equation $Q_{bleed}(t)$ is the volume bleeding rate which includes both the plasma and red blood cells losses. While the loss of RBCs is

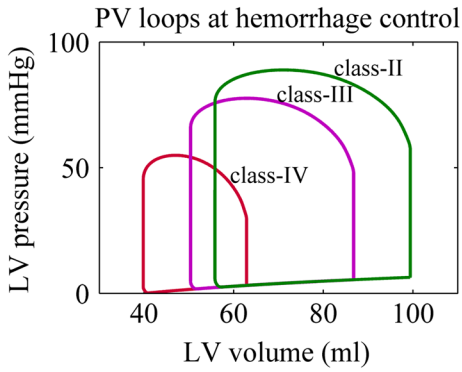

FIGURE A1. Hemodynamic effects of various bleeding classes on left ventricular pressure–volume loop. The hemorrhagic hypovolemia caused a reduction in the preload and stroke volume of the heart compromising its function.

TABLE A1. Model basic equations and symbols list.

Symbol	Meaning	Symbol	Meaning
P_{syst}	Systolic pressure	π_{a_is}	Interstitial arterial-end oncotic pressure
P_{dias}	Diastolic pressure	π_{v_is}	Interstitial venous-end oncotic pressure
D	Diastolic parameter	C_{col_is}	Interstitial colloids concentration
V	Chamber volume	R_{bleed}	Bleeding resistance
x	Chamber index	V_{plasma}	Plasma volume
E	Elastance	V_{RBC}	RBCs volume
π	Oncotic pressure	HCT	Hematocrit
V_{is}	Interstitial fluid volume	HCT_{norm}	HCT initial value[a]
C_{col}	Interstitial colloids concentration	C_{col_B}	Blood total colloids concentration
J_a	Arterial-end fluid transfer rate	$C_{col\_B\_norm}$	Blood proteins initial concentration[a]
J_v	Venous-end fluid transfer rate	Q_{bleed}	Bleeding rate
J_{cap}	Capillary fluid transfer rate	Q_{inf}	Infusion rate
P_{a_cap}	Arterial-end hydrostatic pressure	C_{inf}	Infused colloids concentration
P_{v_cap}	Venous-end hydrostatic pressure	V_{inf}	Infused volume
π_{a_cap}	Capillary arterial end oncotic pressure	R_{exch}	Fluid exchange resistance[a]

Heart chamber systolic and diastolic pressures

$$P_{syst,x}(t) = \max\left(E_{max,x} \cdot E_{N,c}(t_n) \cdot \left(V_x(t) - V_{x,0}\right), 0\right) \quad \text{Eq. (1)}$$

$$P_{diast,x}(t) = D_{1,x} \times 10^{\gamma(D_{2,x})} \cdot e^{(D_{2,x} \cdot V_x(t))} + D_{3,x} \cdot \ln\left(D_{4,x} \cdot V_x(t)\right) \quad \text{Eq. (2)}$$

$$P_x(t) = \max\left(P_{syst,x}(t),\ P_{diast,x}(t)\right) \quad \text{Eq. (3)}$$

Interstitial compartment and fluid exchange

$$P_{is} = \begin{cases} 2.5 \times 10^{-3}\ V_{is} - 37 & \text{for } V_{is} < 14.8\ \text{L}\ [4] \\ 1.0 \times 10^{-4}\ V_{is} - 1.48 & \text{otherwise} \end{cases} \quad \text{Eq. (4)}$$

$$\pi = 0.2274 \cdot C_{col}^2 + 2.1755 \cdot C_{col}\ [4] \quad \text{Eq. (5)}$$

$$J_a(t) = \frac{P_{a\_cap}(t) - P_{a\_is}(t)}{R_{exch}} - \frac{\pi_{a\_cap}(t) - \pi_{a\_is}(t)(t)}{R_{exch}} \quad \text{Eq. (6)}$$

$$J_v(t) = \frac{P_{v\_cap}(t) - P_{v\_is}(t)}{R_{exch}} - \frac{\pi_{v\_cap}(t) - \pi_{v\_is}(t)(t)}{R_{exch}} \quad \text{Eq. (7)}$$

$$J_{cap}(t) = J_a(t) + J_v(t) \quad \text{Eq. (8)}$$

Bleeding equations

$$Q_{bleed}(t) = \frac{P_{a\_cap}(t)}{R_{bleed}} \quad \text{Eq. (9)}$$

$$\frac{dV_{plasma}(t)}{dt} = -Q_{bleed}(t) \cdot (1 - HCT(t)) + J_{cap}(t) \quad \text{Eq. (10)}$$

$$\frac{dV_{RBC}(t)}{dt} = -Q_{bleed}(t) \cdot HCT(t) \quad \text{Eq. (11)}$$

Fluid infusion-controlled hemorrhage

$$\frac{dV_{plasma}(t)}{dt} = Q_{inf}(t) + J_{cap}(t) \quad \text{Eq. (12)}$$

$$C_{col\_B}(t) = \frac{C_{col\_B\_norm} \frac{HCT(t)}{HCT_{norm}} V_{plasma}(t) + C_{inf} \cdot V_{inf}(t)}{V_{plasma}(t)} \quad \text{Eq. (13)}$$

[a]Fluid exchange (bellow).

TABLE A2. Analogous electric circuits of the model elements.

Element	Circuit model
Heart chamber and valve	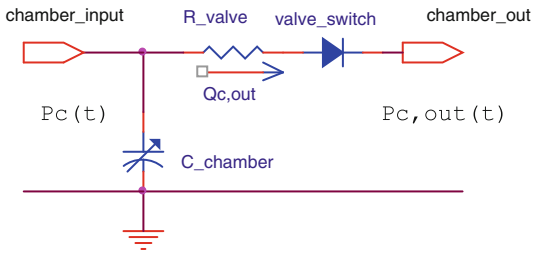
Systemic and pulmonary branches	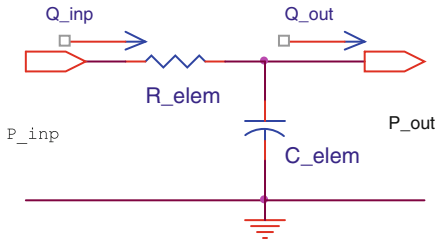
Systemic vein	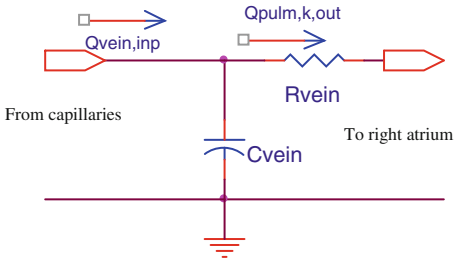
Aortic segment	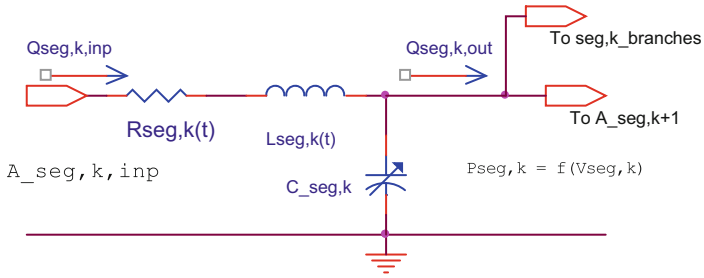
Interstitial fluid–capillary fluid exchange model with bleeding and fluid resuscitation models	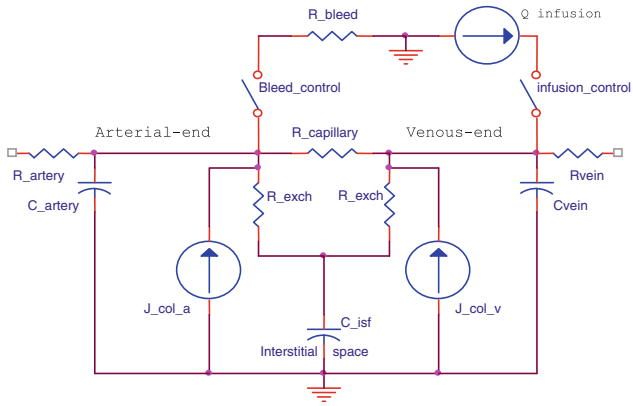

TABLE A3. Normal values of hemodynamic parameters.

Parameter (supine adult at rest)	Normal range	References
Left ventricle		
Systolic	90–140 mmHg	Committee on Fluid Resuscitation for Combat Casualties,[8] p. 17
End-diastolic	6–12 mmHg	Committee on Fluid Resuscitation for Combat Casualties,[8] p. 17
Systemic pressure		
Systolic	90–140 mmHg	Committee on Fluid Resuscitation for Combat Casualties,[8] p. 17
Diastolic	70–90 mmHg	Committee on Fluid Resuscitation for Combat Casualties,[8] p. 17
Hematocrit	38–52%	National Institute for Clinical Excellence "NHS",[21] p. 692

assumed to occur only during hemorrhage, HCT levels are affected both during hemorrhage and fluid resuscitation. The volume loss of red blood cells is computed using Eq. (11).

The blood oncotic pressure is assumed to change with the concentration of colloids according to Eq. (5). The change of blood proteins concentration during both hemorrhage and fluid resuscitation is assumed to be proportional to the value of HCT, it is computed by: $C_{\text{col\_B}}(t) = C_{\text{col\_B\_norm}} \cdot \frac{HCT(t)}{HCT_{\text{norm}}}$ (Eq. (12),[1]), where $C_{\text{col\_B\_norm}} = 7.3\%$ and $HCT_{\text{norm}} = 44\%$. The total weight of blood proteins is computed by $W_{\text{prot\_B}}(t) = C_{\text{col\_B}}(t) \cdot V_{\text{plasma}}(t)$.

During treatment with colloid fluids, the plasma colloids concentration is increased according to the fluid infusion rate. The weight of infused colloids is $W_{\text{col\_B\_inf}}(t) = C_{\text{inf}} \cdot V_{\text{inf}}(t)$. The concentration of blood colloids, in the case of controlled hemorrhage and treatment with colloid fluids, is computed by: $C_{\text{col\_B}}(t) = \frac{W_{\text{prot\_B}}(t) + W_{\text{col\_B\_inf}}(t)}{V_{\text{plasma}}(t)}$. In this expression $V_{\text{plasma}}(t)$ was computed by the integration of Eq. (12) which takes into account the combined effect of fluid infusion and exchange with the interstitial space.

Fluid exchange between the intravascular and interstitial compartments is computed as the net filtration of fluid at the arterial and venous ends of the capillary (Eq. (8)). The fluid is assumed to flow between the two compartments through a fluid exchange resistance $R_{\text{exch}} = 25$ mmHg s/mL.[13] Which is taken as constant and equal for both capillary sides. The flow of fluid at each capillary side is composed of two components, the first component is proportional to the hydrostatic pressure difference, while the second component is proportional to the oncotic pressure difference between the intravascular and interstitial compartments (Eqs. (6) and (7)).

CONFLICT OF INTEREST

No benefits in any form have been or will be received from a commercial party related directly or indirectly to the subject of this manuscript. Jamal Siam, Yossi Mandel and Ofer Barnea declare that they have no conflict of interest.

REFERENCES

[1]American College of Surgeons. Advanced Trauma Life Support for Doctors (8th ed.). Chicago: American College of Surgeons, 2008.

[2]Barnea, O., and N. Sheffer. A computer model for analysis of fluid resuscitation. *Comput. Biol. Med.* 23(6):443–454, 1993.

[3]Baue, A., *et al.* Hemodynamic and metabolic effects of Ringer's lactate solution in hemorrhagic shock. *Ann. Surg.* 166(29–38):1, 1967.

[4]Boyers, G., *et al.* Simulation of the human cardiovascular system: a model with normal response to change of posture, blood loss, transfusion, and autonomic blockade. *Simulation* 18:197–206, 1972.

[5]Bruttig, S., *et al.* Benefits of slow infusion of hypertonic saline/dextran in swine with uncontrolled aortotomy hemorrhage. *Shock* 1(24):92–96, 2005.

[6]Choi, P., *et al.* Crystalloids versus colloids in fluid resuscitation: a systematic review. *Crit. Care Med.* 27:200–210, 1999.

[7]Civetta, J. A new look at the Starling equation. *Crit. Care Med.* 7(3):84–91, 1979.

[8]Committee on Fluid Resuscitation for Combat Casualties. Fluid Resuscitation: State of the Science for Treating Combat Casualties and Civilian Trauma Report of the Institute of Medicine. Washington: National Academy Press, 1999.

[9]Finfer, S., *et al.* A comparison of albumin and saline for fluid resuscitation in the intensive care unit. *N. Engl. J. Med.* 350:2247–2256, 2004.

[10]Guyton, C., and T. Coleman. Quantitative analysis of pathophysiology of hypertension. *Circ. Res.* 269(10), 1963.

[11]Gyenge, C., *et al.* Transport of fluid and solutes in the body I. Formulation of a mathematical model. *Am. J. Physiol. Heart Circ. Physiol.* 277:215–227, 1999.

[12]Gyenge, C., *et al.* Transport of fluid and solutes in the body II. Validation and implications. *Am. J. Physiol. Heart Circ. Physiol.* 277:1228–1240, 1999.

[13]Hedlund, A., B. Zaar, T. Groth, and G. Arturson. Computer simulation of fluid resuscitation in trauma. I. Description of an extensive pathophysiological model and its first validation. *Comput. Methods Programs Biomed.* 27(1):7–21, 1988.

[14]Kramer, G., *et al.* Small-volume resuscitation with hypertonic saline dextran solution. *Surgery* 2(100):239–247, 1986.

[15]Kwan, I. Timing and volume of fluid administration for patients with bleeding. *Cochrane Database Syst. Rev.* Art. No. CD002245(3), 2003.
[16]Lentner, C. Geigy Scientific Tables-Heart and Circulation (8th ed.)., Vol. 5. Basel: CIBA-GEIGY, 1990.
[17]Lodi, C., and M. Ursino. Hemodynamic effect of cerebral vasospasm in humans: a modeling study. *Ann. Biomed. Eng.* 27:257–273, 1999.
[18]Mardel, S., *et al.* Validation of a computer model of haemorrhage and transcapillary refill. *Med. Eng. Phys.* 17(3):215–218, 1995.
[19]Mazzoni, M., *et al.* Dynamic fluid redistribution in hyperosmotic resuscitation of hypovolumic hemorrhage. *Am. J. Physiol.* 255:629–637, 1988.
[20]Milnor, W. Cardiovascular Physiology (1st ed.). New York: Oxford University Press, 1990.
[21]National Institute for Clinical Excellence "NHS". Prehospital Initiation of Fluid Replacement Therapy in Trauma, Issue 2004. London: National Institute for Clinical Excellence, 2007.
[22]Pati, S., *et al.* Protective effects of fresh frozen plasma on vascular endothelial permeability, coagulation, and resuscitation after hemorrhagic shock are time dependent and diminish between days 0 and 5 after thaw. *Trauma* 69:55–63, 2010.
[23]Pryke, S. Advantages and disadvantages of colloid and crystalloid fluids. *Nurs. Times* 100(10):32–33, 2004.
[24]Riddez, L., *et al.* Lower dose of hyper-tonic saline dextran reduces the risk of lethal rebleeding in uncontrolled hemorrhage. *Shock* 5(17):377–382, 2002.
[25]Rizoli, S. Crystalloids and colloids in trauma resuscitation: a brief overview of the current debate. *Trauma* 54:S82–S88, 2003.
[26]Ryan, M., *et al.* Initial hematocrit in trauma: a paradigm shift? *J. Trauma Acute Care Surg.* 72:54–59, 2012.
[27]Secomb, T. Theoretical models for regulation of blood flow. *Microcirculation* 15(8):765–775, 2008.
[28]Secomb, T., *et al.* Two-dimensional simulation of red blood cell deformation and lateral migration in microvessels. *Ann. Biomed. Eng.* 35(5):755–765, 2007.
[29]Simpson, S., *et al.* A computer model of major haemorrhage and resuscitation. *Med. Eng. Phys.* 18(4):339–343, 1996.
[30]Stern, S., *et al.* Comparison of the effects of bolus vs. slow infusion of 7.5% NaCl/6% dextran-70 in a model of near-lethal uncontrolled hemorrhage. *Shock* 6(14):616–622, 2000.
[31]Stevens, S., and W. Lakin. A mathematical model of the systemic circulation system with logistically defined nervous system regulatory mechanisms. *Math. Comput. Model. Dyn. Syst.* 12(6):555–576, 2006.
[32]Trebbels, D., *et al.* Hematocrit measurement—a high precision on-line measurement system based on impedance spectroscopy for use in hemodialysis machines. *World Congr. Med. Phys. Biomed. Eng.* 25:247–250, 2009.
[33]Ursino, M., and E. Magosso. Role of tissue hypoxia in cerebrovascular regulation: a mathematical modeling study. *Ann. Biomed. Eng.* 29:563–574, 2001.
[34]Westerhof, H., *et al.* Snapshots of Hemodynamics (2nd ed.). New York: Springer, 2010.
[35]World Health Organization. Violence, Injuries, and Disabilities Biennial Report 2008–2009. WHO Library Cataloguing-in-Publication Data, 2010.
[36]Yitzchak, A., *et al.* Hematocrit and metabolic changes caused by varied resuscitation strategies in a Canine model of hemorrhagic shock. *Am. J. Emerg. Med.* 20:303–309, 2002.